A new and efficient way to construct synthetic porous fractured or heterogeneous medium

Leo Kirchhof Santos (Faculdade de Geofísica-UFPA), José J. S. de Figueiredo (Faculdade de Geofísica-UFPA e INCT-GP), Daniel L. Macedo (Faculdade de Geofísica-UFPA), Alberto L Melo (Faculdade de Geofísica-UFPA) & Carolina Barros da Silva (Faculdade de Geofísica-UFPA),

Abstract

Fractures occur in the earth under wide range of scales and in different depths. Understand them from wave propagations, is a hard task, which has consumed plenty of research time both in the oil industry and academy. Many authors have been investigating the behaviour of seismic waves in fractured media through the use of physical modelling, which several methods for synthetic sample preparation has been used. We have developed a new, efficient and feasible methodology of fractured sample construction, based on: cement, sand, especial material (cuts holder) and solvent. The cuts holder (material A) (square piece or penny-shape) are leached out by using solvent B. The empty space created by this leaching can represent fractures or cracks in a porous background. The sample petrophysical parameters are controlled by pressure, temperature and clay content, or in this work by the cement content. To verify the feasibility of our methodology, P- and S-wave ultrasonic velocities and Thomsen anisotropy parameters (ε and γ) were estimated in four dry fractured samples and in a reference sample. Purposely, our reference sample has a background anisotropy induced by layer-by-layer material deposition. The results show a coherent behaviour of anisotropy parameter as function of number of dry fractures. This new methodology highlights the possibility of using less expensive materials and in a short time to construct anisotropic media made by fractured or cracked regions.

Introdução

The study of rocks in reduced scale has been very helpful in the analyses of the influence of different geological features in the seismic wave. The use of synthetic rocks that physically reproduce the characteristics of real rocks, with all their particularities, such as porosity, different crack physical parameters (crack density, aspect ratio, crack orientation, etc.) and mineralogy, instead of numerical simulation, brings more complete and reliable information in the study of the seismic waves propagation, since the waves are affected by artifacts similar to the ones present in real rocks. Many authors have been studying different ways to reproduce rocks in reduced scale. Assad et al. (1993,1996) created synthetic anisotropic samples composed by epoxy resin with penny-shaped rubber inclusions to study the influence of different crack geometries in P- and S- waves and compared their results with the effective model proposed by Hudson et al. (1981). Similar way to construct anisotropic samples was performed by De Figueiredo et al. (2012, 2013) and Santos et al. (2015), that proposed other types of analyses in the synthetic samples. These epoxy made samples have great utility to investigate the effect of different crack characteristics in elastic wave propagation. However, these samples have some limitations in the context of primary porosity, that can't be reproduced using epoxy as the matrix composition.

To achieve more reliability for the synthetic rocks and enable different types of analyses, some authors have been creating new sample production methodologies. Santos et al. (2016) created porous synthetic sandstones whose matrices were produced by a mixture of sand and cement. Rathore et al. (1995) produced synthetic porous sandstones made by sand and epoxy resin. Tillotson et al. (2012) used the same method to create cracked samples as described by Rathore et al. (1995), however, they developed a way to produce synthetic sandstones without the use of resin as a binder for the samples. These samples are a result of the mixture of sand, kaolinite and sodium silicate, that acquire consistence when put in contact with high temperatures. A similar approach for cracked synthetic rocks production was performed by Amalokwu et al. (2014, 2015, 2016), where they studied the effects of rock saturation in seismic waves. Ding et al. (2014a, 2014b) used a new construction method to produce synthetic samples using a mixture of sand, clay, feldspar and sodium silicate. Also, they used high molecular discs that were decomposed after the samples were put in a high temperature furnace.

The chemical leaching of aluminum discs by acid is a robust method to make penny-shaped voids. Also, the construction methods of silica-cemented sandstones described above are well accepted as reliable synthetic rocks. However, these methods have some punctual negative factors that could be improved. For example, in the construction method of Ding et al. (2014a, 2014b) the samples remained in a constant temperature oven for several days, turning the process very slow. The method of leaching the metallic discs with acid is not efficient for a synthetic rock composed by calcite or dolomite, since this material react with acid. In our approach, we propose a

new simple and efficient construction methodology of porous fractured samples, using a mixture of cement and sand with controlled proportions as the components of the rock matrix and very cuts holder, after being dissolved by solvent B, leave empty shapes inside the samples representing fractures. We test the applicability of this methodology estimating P- and S-wave velocity and anisotropy in four fractured samples with controlled and different fracture characteristics.

Metodologia

The construction of the synthetic rock samples as well as the ultrasonic measurements were performed at the Laboratory of Petrophysics and Rock Physics – Dr. Om Prakash Verma (LPRP) at the Federal University of Pará, Brazil. The following methodology description corresponds to the production of fractured synthetic sandstones.

Fractured sample preparation methodology

The first step was to create the cuts A that simulate the fractures in the samples. In this work we used square-shaped cuts but the same process can be realized using discs or other geometries. After this, we prepared the materials used as the constituents of the samples background, which are sifted clean sand and cement. We sifted the clean sand to ensure a size distribution ranging from 50 to 300 μm. These components are manually mixed in order to ensure homogeneity. We inserted water in the grain mixture, which acts as the element that turn the matrix stiff.

After the grain mixture preparation, a certain amount of it is poured in an acrylic box that acts as the mould for the samples. This mould is lubricated with vaselin to facilitate the sample removal when it is done. To create the fracture planes, we put squared cuts on the top of each layer, a process repeated until the desired number of fracture planes was achieved. Each layer was submitted to a hydrostatic vertical static stress of approximately 0.01 MPa performed by a hydraulic in order to flat them. This process of layer production utilizing applied pressure causes a preferential grain orientation in each of the layer, causing intrinsic anisotropy in the isotropic background. The same issue occurred in Tillotson et al. (2012). The pressure was applied only in the process of sample construction, to reach more compacted synthetic rocks, not being used in the process of ultrasonic measurements. After the construction, all the samples were put in a heater device in order to get them dry. The temperature applied was 100 ^{O}C which is not enough to melt the material A. In order to decrease possible composition and density difference among the samples, they were constructed simultaneously, using the same material mixture.

The final step is to immerse the blocks in a solvent B, which is a solvent that percolates the porous rocks and dissolves the cuts, leaving out squared shaped voids that represent fractures (see Figure A). One great advantage of paint thinner is the fact that it does not require a very porous rock to percolate. Another advantage is the fact that its use as the chemical leaching does not cause chemical reaction between it and the matrix, which is very important in the context of carbonate samples construction. It is important to highlight that all the process can be reproduced with other mineralogical components, such as calcite, dolomite, clay, etc.

The samples used in this work represent four sandstones with series of fracture planes, with controlled fracture number, dimension, separation and density. A mixture of sifted clean sand and cement, with a fixed proportion of 35% and 65%, composes their matrices respectively. We chose this proportion for the matrix to provide strength, water insolubility and a reasonable porosity. The fractures are represented by thin squared voids generated after the dissolution of cuts A. We created four samples with different separation between fracture planes, resulting in four synthetic rocks with VTI symmetry and different fracture densities. The overall characteristics of each fractured sample are depicted in Table 1. The samples porosities were estimated by saturating the samples with water and measuring the difference between dry and saturated masses. Considering the water density equals 1gm/cm³, this difference is considered the volume of empty spaces in the samples, which allowed us to estimate the porosities along with the total volume of the samples. The fracture density is estimated by the following equation:

$$\epsilon = N\frac{Vf}{Vt}$$

where N is the total number of fractures, Vf is the volume of an individual fracture and Vt is the volume of the space occupied by the fractures.

Table 1 - Physical parameters of reference and fractured samples. Precision of length measurements was about 0.02 cm.

Sample	Measuring Length model (cm) Lx	Lz	Number of fractures	Fracture plane separation (cm)	Average fracture density (%)	Primary Porosity (%)	Fracture porosity (%)
REF	6,2	5,97	0	0	0	10.45	0
CI - 1	6,32	5,87	10	0,5	21	10.33	16.7
CI - 2	6,39	5,83	5	1,0	12,5	10.02	9.1
CI - 3	5,97	6,02	4	1,5	8,8	10.10	6.25
CI - 4	6,01	6,24	3	2,0	7,5	10.26	4.27

Figure 3: The heterogeneous models related to groups A and B and the reference model.

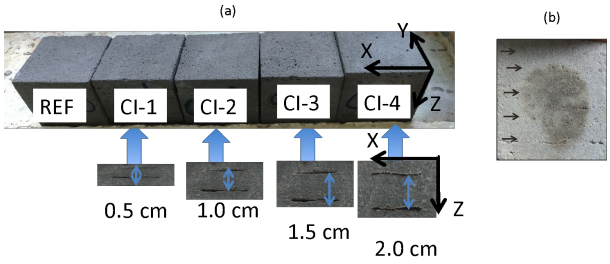

Figure 2 – a) From left to right: photograph of the reference sample (REF) and fractured samples CI-1 to CI-4. Below, from left to right: description of fracture plane separation of the four fractured samples. (b) This picture shows layer contact that can induce anisotropy even in the case of a reference sample. Figures 2 shows the anisotropy magnitude for the unfractured rock (reference sample).

Ultrasonic measurements

The ultrasonic measurements were realized using the Ultrasonic Research System at LPRF with the pulse transmission technique. The sampling rate per channel for all measures of S-wave records was 0.1 μs. The system consists of: a pulse-receiver 5072PR and pre-amplifier 5660B from Olympus, a S-wave transducer of 500 KHz also from Olympus and a USB oscilloscope of 50 MHz from Handscope. The S-wave transducer has an intrinsic delay time of 0.14 μs in its signal, being necessary to take this delay into consideration when estimating the wave velocities. This intrinsic delay is due the space that exists between the crystal that generates the waves and the core that protects the whole system of the transducers. The complete description of this setup is described in Santos et al. (2015).

We arranged the source and receiver transducers on opposing sides of the synthetic rocks, separated by their lengths. To ensure that the wave propagation was in the desired region of the rocks, we placed the transducers at the centre of both sides and measured the velocities in the longitudinal direction. We performed the transmission measures using a 500 KHz S-wave transducer that allows the estimative of both P and S-waves first arrivals from a single waveform. Knowing the dimensions of the blocks, we could estimate P and S-wave velocities. The same procedure was repeated parallel and perpendicular to the fault planes. In the case of the fractured samples, the direction parallel to the fault planes is called X direction, while the direction perpendicular to the fault planes is called Z direction. In order to quantify the P-wave and S-wave anisotropies, we estimated the parameters ε (related to P-waves) and γ (related to S-waves), based on equations proposed by Thomsen (1984)

$$\varepsilon = \frac{Vp1^2 - Vp2}{2Vp1^2},$$
$$\gamma = \frac{Vs2^2 - Vs2^2}{2Vs2^2}$$

where Vp1 and Vp2 are the P-wave velocities parallel and perpendicular to the fault planes, respectively, and Vs1 and Vs2 are the S-wave velocities for polarizations parallel and perpendicular to the fault planes, respectively.

Results

In order to show that this proposed methodology of fractured samples construction is efficient, we performed some analyses to ensure if the constructed samples present a VTI behavior caused by the fractures. As said before, the samples from CI-1 to C1-4 are the fractured samples, with fracture number decreasing from sample CI-1 to sample CI-4, while the reference sample is isotropic. As explained before, we estimated the P- and S-wave velocities from the dimensions of the blocks and the waves travel times. These first arrivals were estimated from the first breaks of the fast and slow P- and S-waves. The variation of both fast P-wave (X-direction) and slow P-wave (Z-direction) velocities for the different samples is depicted in Figure 2a). As expected, the fast P-wave velocities have just a little variation for different fracture densities. In comparison with the slow P-wave velocities they are less affected with the variation of fracture number. On the other hand, the slow P-wave velocities have a difference of more than 300m/s between the lower and faster velocities. This wave is highly affected by the fractures because it directly crosses the fractures, being highly attenuated. Since the sample CI-1 has the highest number of fractures, its slow P-wave velocity is the lowest among all the samples. The fast S-waves have their polarization parallel to the fracture planes, being poorly affected by them, while the slow S-wave has its polarization perpendicular to the fracture planes. The highest the fracture density, the lower is the slow S-wave velocity, as can be observed in Figure 2b). The behavior of the anisotropic parameters is the opposite of the P- and S-wave velocities. Both the P-wave and S-wave anisotropic parameters decreases with the increasing fracture density. These behaviors are depicted in Figure 2 c).

Figures 4.a and 4.b show the variation of anisotropic parameters γ and ε as a function of parameters $\sum_P$ and $\sum_S$. The parameters are defined as

$$\sum_P = \frac{\lambda_p}{d},$$
$$\sum_S = \frac{\lambda_S}{d},$$

where λ_P and λ_S are the dominant wavelength of P-wave propagating perpendicular to the fault planes and S-wave with polarization perpendicular to the fault planes, respectively, while d is the plane faults average separation. They are calculated for each fractured sample. They are analyzed in order to ensure if the estimated anisotropy parameters values are proportional to the number of fractures enclosed by a single wavelength. Both Figures show that the parameters ε and γ are directly proportional to the values of $\sum_P$ and $\sum_S$, being the highest values of both $\sum_P$ and $\sum_S$ associated with the highest anisotropic parameters values. We realized data fitting in both of the analyses, extrapolating

the fitting curves until the point where both $\sum_P$ and $\sum_s$ correspond to zero, which are considered the values for the reference sample. The Figures show a very similar result for the calculated parameters and extrapolating values for the reference sample.

Conclusions

In this work, we have developed new methodology to construct synthetic anisotropic models. Our test with this new methodology was very successful, being proved that the dissolved cuts of a material A generate empty spaces inside the samples. Also, numerous advantages of the proposed methodology were shown, as the fact that it can be used for any mineralogical composition and it does not require a high porosity matrix to achieve the cuts A dissolution. The results of the variation of P- and S-wave velocities and anisotropic parameters as a function of the fracture density, as well as the analyses of $\sum_P$ and $\sum_s$, showed that the built fractured samples provide practical results. This methodology proved to be a cheap, simple and efficient method of fractured sample construction. Because of the simplicity of the process and cuts A modeling capacity, this new method can be used to create more complex types of fractured samples with a certain easiness, such as orthorhombic media and synthetic carbonate rocks without restrictions.

Acknowledgements

The authors would like to thank CAPES, INCT-GP and CNPq (Grant No.: 4590653/2014-6 and Grant No.: CNPQ 140174/2016-8) from Brazil and the graduate program at Federal University of Pará for the financial support in this research.

References

Assad, J. M., J. A. Mcdonald, R. H. Tatham, and T. M. Kusky, 1996, Elastic wave propagation in a medium containing oriented inclusions with a changing aspect ratio: A physical model study: Geophysical Journal International, 125, 163–172.

Assad, J. M., R. H. Tatham, J. A. Mcdonald, T. M. Kusky, and J. Jech, 1993, A physical model study of scattering of waves by aligned cracks: Comparison between experiment and theory1: Geophysical Prospecting, 41, 323–339.

Amalokwu, K., A. I. Best, J. Sothcott, M. Chapman, T. Minshull, and X. Y. Li, 2014, Water saturation effects on elastic wave attenuation in porous rocks with aligned fractures: Geophysical Journal International, 197, 943–947.

Amalokwu, K., M. Chapman, A.I. Best, J. Sothcott, T.A. Mishul, X.Y. Li, 2015, Experimental observation of water saturation effects on shear wave splitting in synthetic rock with fractures aligned at oblique angles, Geophys. J. Int., 200, 17–24.

Amalokwu, K., Angus I. Best and Mark Chapman, 2016, Effects of aligned fractures on the response of velocity and attenuation ratios to water saturation variation: a laboratory study using synthetic sandstones, Geophysical Prospecting, 64, 942–957.

Crampin, S. (1984), Effective anisotropic elastic constants for wave propagation through cracked solids. *Geophys. J. Roy. Astr. Soc.*, 76, 135-145.

De Figueiredo, J. J. S., J. Schleicher, R. R. Stewart, and N. Dyaur, 2012, Estimating fracture orientation from elastic-wave propagation: An ultrasonic experimental approach: Journal of Geophysical Research: Solid Earth, 117, B08304.

De Figueiredo, J. J. S., J. Schleicher, R. R. Stewart, N. Dayur, B. Omoboya, R. Wiley, and A. William, 2013, Shear wave anisotropy from aligned inclusions: ultrasonic frequency dependence of velocity and attenuation: Geophysical Journal International, 193, 475– 488.

Ding, P., B. Di, D. Wang, J. Wei, and X. Li, 2014a, P and S wave anisotropy in fractured media: Experimental research using synthetic samples: Journal of Applied Geophysics, 109, 1–6.

Ding, P., B. Di, J. Wei, X. Li, and Y. Deng, 2014b, Fluid-dependent anisotropy and experimental measurements in synthetic porous rocks with controlled fracture parameters: Journal of Geophysics and Engineering, 11, 015002.

Eshelby, J. D. (1957), The determination of the elastic field of an ellipsoidal inclusion, and related problems. *Proc. Royal Soc. London A*, v. 241, p. 376–396.

Far, M. E., J. J. S. de Figueiredo, R. R. Stewart, J. P. Castagna, D.-H. Han, and N. Dyaur, 2014, Measurements of seismic anisotropy and fracture compliances in synthetic fractured media: Geophysical Journal International, 197, 1845–1857.

Hudson, J. A. (1981), Wave speeds and attenuation of elastic waves in material containing cracks. *Geophys. J. R. Astron. Soc.*, v. 64, p. 133-150.

Hudson, J. A. and Liu, E. (1999), Effective elastic properties of heavily faulted structures. *Geophysics*, v. 64, n. 2, p.479-489.

Nishizawa, O. (1982). Seismic velocity anisotropy in a medium containing oriented cracks-transversely isotropic case. *Journal of Phys. Earth* 30, 331-347.

Rathore, J. S., E. Fjaer, R. M. Holt, and L. Renlie, 1995, P- and S-wave anisotropy of a synthetic sandstone with controlled crack geometry: Geophysical Prospecting, 43, 711–728.

Santos, L. K., J.J.S. de Figueiredo , Bode Omoboya, Jörg Schleicher, Robert R. Stewart, Nikolay Dyaur, 2015, On the source-frequency dependence of fracture-orientation estimates from shear-wave transmission experiments, Journal of Applied Geophysics, 114, 81–100.

Santos, L. K., J.J.S. de Figueiredo , Carolina B. da Silva, 2016, A study of ultrasonic physical modeling of isotropic media based on dynamic similitude, Ultrasonics, 70, 227–237.

Stewart, R. R., N. Dyaur, B. Omoboya, J. J. S. de Figueiredo, M. Willis, and S. Sil, 2011,Physical modeling of anisotropic domains: Ultrasonic imaging of laser-etched fractures in glass: , 2865–2869.

Thomsen, L. (1995), Elastic anisotropy due to aligned cracks in porous rock. *Geophysical Prospecting* 43, 805–

829.
Thomsen, L. (1986), Weak elastic anisotropy. *Geophys.*, v. 51, p. 1954–1966.
Tillotson, P., J. Sothcott, A. I. Best, M. Chapman, and X.-Y. Li, 2012, Experimental verification of the fracture density and shear-wave splitting relationship using synthetic silica cemented sandstones with a controlled fracture geometry: Geophysical Prospecting, 60, 516–525.
Wang, Z., Ruihe Wang, Feifei Wang, Hao Qiu , and Tianyang Li, 2015, Experiment study of pore structure effects on velocities in synthetic carbonate rocks: Geophysics, 80, D207–D219.

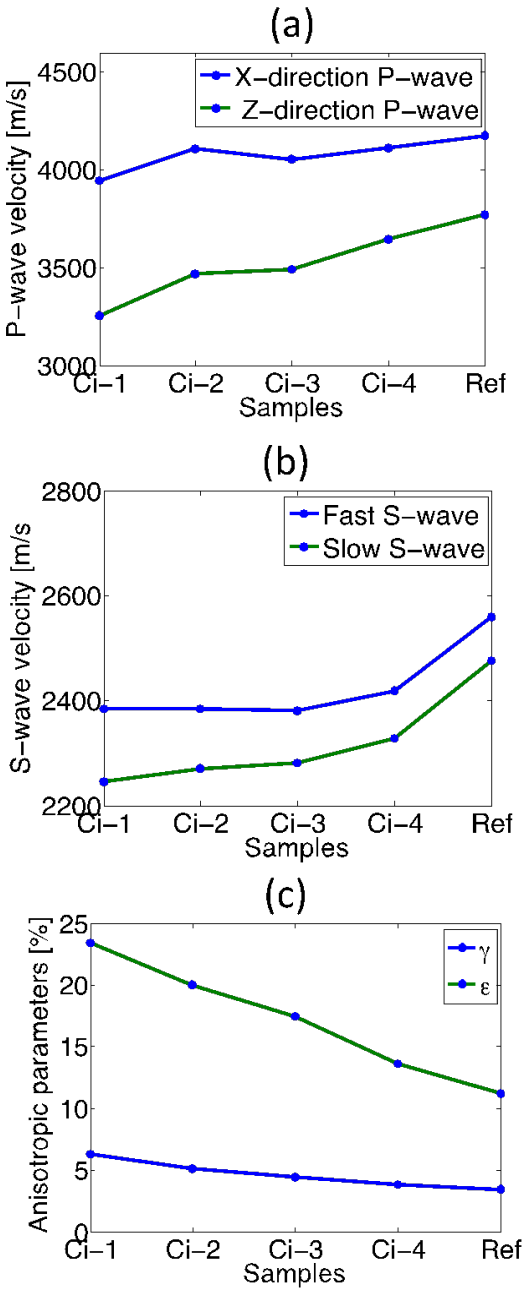

Figure 3. (a) P-wave velocities, (b) S-wave velocities in Z and X directions for all samples and (c) P- and S-wave anisotropic parameters for all samples.

(a)

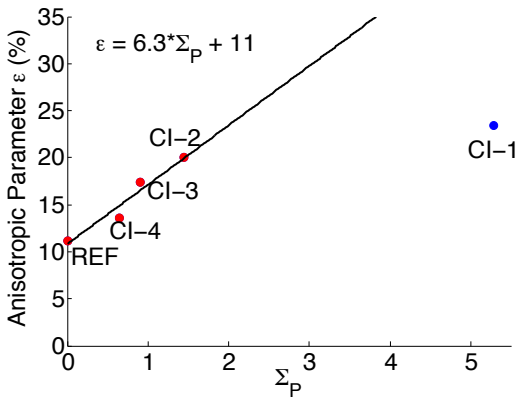

(b)

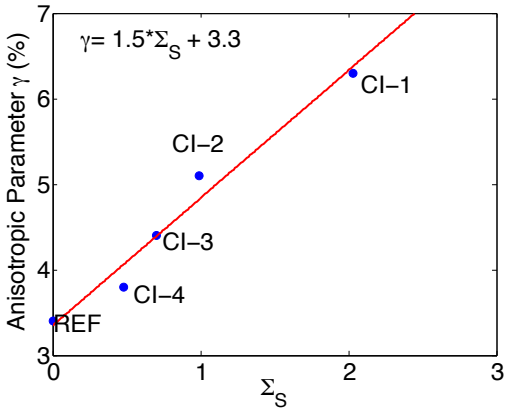

Figure 4. a) Σ_P variation with ε and the linear fitting of the points and b) $\sum_S$ variation with ε and the quadratic fitting of the points.